ACS APPLIED BIO MATERIALS

Article

Cite This: ACS Appl. Bio Mater. 2018, 1, 1319−1327

www.acsabm.org

A Layer-by-Layer Approach To Retain a Fluorescent Glucose Sensing Assay within the Cavity of a Hydrogel Membrane

Andrea K. Locke,[†] Anna Kristen Means,[‡] Ping Dong,[†] Tyler J. Nichols,[†] Gerard L. Coté,[†,∥] and Melissa A. Grunlan*[,†,‡,§,∥]

[†]Department of Biomedical Engineering, [‡]Department of Materials Science and Engineering, [§]Department of Chemistry, and [∥]Center for Remote Healthcare Technologies, Texas A&M University, College Station, Texas 77843-3120, United States

ABSTRACT: A continuous glucose monitoring device that resides fully in the subcutaneous tissue has the potential to greatly improve the management of diabetes. Toward this goal, we have developed a competitive binding glucose sensing assay based on fluorescently labeled PEGylated concanavalin-A (PEGylated-TRITC-ConA) and mannotetraose (APTS-MT). In the present work, we sought to contain this assay within the hollow central cavity of a cylindrical hydrogel membrane, permitting eventual subcutaneous implantation and optical probing through the skin. A "self-cleaning" hydrogel was utilized because of its ability to cyclically deswell/reswell in vivo, which is expected to reduce biofouling and therefore extend the sensor lifetime. Thus, we prepared a hollow, cylindrical hydrogel based on a thermoresponsive electrostatic double network design composed of *N*-isopropylacrylamide and 2-acrylamido-2-methylpropanesulfonic acid. Next, a layer-by-layer (LbL) coating was applied to the inner wall of the central cavity of the cylindrical membrane. It consisted of 5, 10, 15, 30, or 40 alternating bilayers of positively charged poly(diallyldimethylammonium chloride) and negatively charged poly(sodium 4-styrenesulfonate). With 30 bilayers, the leaching of the smaller-sized component of the assay (APTS-MT) from the membrane cavity was substantially reduced. Moreover, this LbL coating maintained glucose diffusion across the hydrogel membrane. In terms of sensor functionality, the assay housed in the hydrogel membrane cavity tracked changes in glucose concentration (0 to 600 mg/dL) with a mean absolute relative difference of ∼11%.

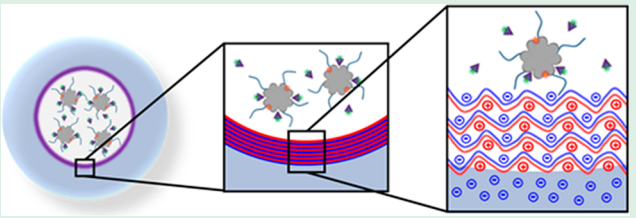

KEYWORDS: *layer-by-layer, hydrogel, thermoresponsive, biosensor, glucose*

INTRODUCTION

Diabetes mellitus affects more than 29 million people in the U.S. and over 300 million people worldwide.[1] Tight glycemic control is of critical importance, as hyper- and hypoglycemic states can lead to short and long-term complications as well as morbidity.[1,2] The commonly used finger-prick test provides only intermittent monitoring and is associated with poor testing compliance stemming from its inconvenience and discomfort. Continuous glucose monitors (CGMs), by providing real-time glycemic monitoring, have the potential to improve diabetes management and health outcomes.[3−5] Current FDA-approved CGMs are based on an electroenzymatic sensor consisting of a needle-type probe comprised of an electrode and embedded glucose oxidase enzyme. The probe is transdermally inserted, and the glycemic level in the interstitial fluid (ISF) is monitored via amperometric signals from the glucose oxidation reaction. While some newer CGMs have eliminated finger-prick test calibrations, the sensors must be replaced every 7−10 days. Their transdermal nature is required for frequent removal and replacement but also is associated with irritation and infection at the insertion site.[6] A CGM that could achieve a longer lifetime and thus be implanted fully subcutaneously would represent a significant advancement. To achieve this, progress must be made to improve glucose sensing as well as to reduce sensor biofouling. Toward the realization of a subcutaneous CGM, we have conducted independent studies on an optical glucose sensing assay and a self-cleaning sensor membrane as described below and in Figure 1.

Optical glucose biosensors are advantageous over electrochemical sensors because they do not rely on the placement of a transducer or other hardware components in direct contact with the specimen during sensing, thereby allowing for the potential development of non- or minimally invasive biosensors. Various optical glucose monitoring approaches have been reviewed in the literature.[7−9] Those based on the use of optical modalities include Raman spectroscopy,[10−14] optical coherence tomography (OCT),[15,16] photoacoustic spectroscopy,[17−19] optical polarimetry,[20−24] infrared spectroscopy,[25,26] and fluorescence spectroscopy.[27−31]

Competitive binding assays to track glucose levels using Förster resonance energy transfer (FRET) as the transduction mechanism that are based on concanavalin A (ConA) (a glucose receptor) and a glucose-like competing ligand have been described.[32−37] At pH 7.4, ConA comprises four identical monomeric subunits,[38] each of which has a single carbohydrate

Received: June 25, 2018
Accepted: October 10, 2018
Published: October 10, 2018

DOI: 10.1021/acsabm.8b00267
ACS Appl. Bio Mater. 2018, 1, 1319−1327

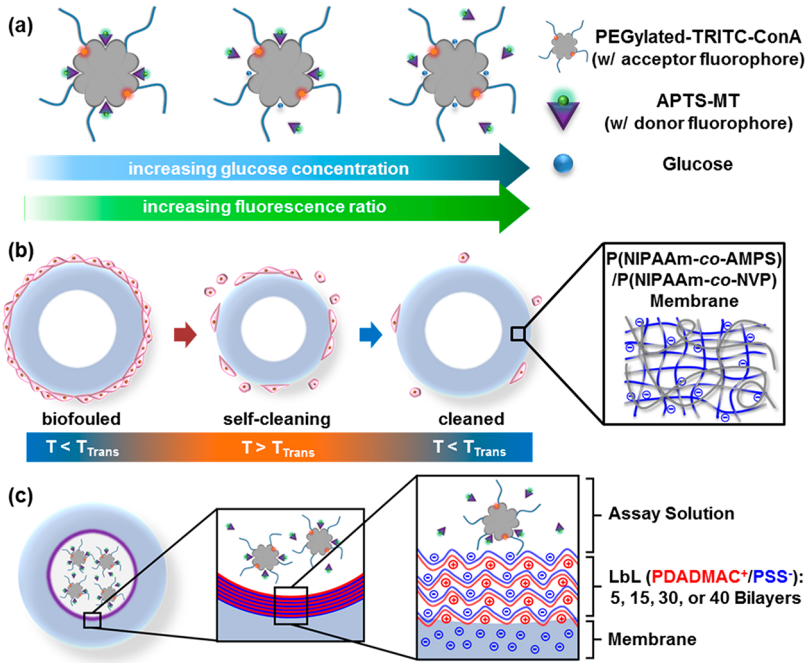

Figure 1. (a) Fluorescent competitive binding assay based on PEGylated-TRITC-ConA and APTS-MT. (b) Cross-section of self-cleaning membrane "cylinder" with a hollow cavity. (c) LbL coating applied to the membrane cavity wall to inhibit diffusion of the assay components from the cavity.

binding site. ConA is able to reversibly bind to glucose (with high affinity) and a fluorescently labeled competing ligand (presenting multiple low-affinity moieties) (e.g., fluorescein isothiocyanate (FITC)-dextran). Thus, changes in the fluorescence signal at equilibrium can be used to observe the concentration of glucose. However, these assays are prone to aggregation in free solution, a result of extensive cross-linking between the multiple binding sites of ConA and the multivalent competing ligand, as well as the inherent thermal instability of ConA.[31,39,40] Thus, we recently reported the use of a new type of competing ligand, aminopyrene trisulfonate mannotetraose (APTS-MT), which presents a single high-affinity trimannose moiety that utilizes the full binding site of ConA and thus avoids aggregation.[41] Additionally, we demonstrated that tethering of poly(ethylene glycol) (PEG) to ConA (i.e., PEGylation) improved ConA's thermal stability and resistance to electrostatic binding.[42] Finally, we demonstrated improved FRET efficiency leading to enhanced sensitivity to changes in glucose levels.[43] Compared with APTS-dextran, the close proximity of APTS-MT's core trimannose structure and donor fluorophore decreases the distance between the FRET donor and FRET acceptor on ConA to maximize the FRET efficiency upon binding of the ligand to ConA. Thus, as the glucose concentration increases, the ratio of the fluorescence intensities of the two dyes (520 to 580 nm) would be expected also to increase because of an increase in the Förster radius during the competition between glucose and APTS-MT for the binding sites of ConA (Figure 1a). Thus, in free solution the FRET efficiency of the assay increased from ∼25% with APTS-dextran to ∼89% with APTS-MT across the physiologically relevant glucose range and thus had 4 times more sensitivity.[43] This PEGylated-TRITC-ConA/APTS-MT assay in free solution also displayed a mean absolute relative difference (MARD) of 5% across the physiologically relevant glucose concentration range.

We have also previously described "self-cleaning" membranes directed at reducing biofouling on implanted glucose biosensors (Figure 1b).[44−46] These membranes are based on poly(*N*-isopropylacrylamide) (PNIPAAm) hydrogels, which are known to undergo reversible deswelling/reswelling when cycled above/below their volume phase transition temperature (VPTT).[47,48] This process has been applied to thermally control the removal of cultured cells in vitro.[49−51] Transdermal heating/cooling or body temperature fluctuations may affect thermal cycling of such an implanted membrane. Most recently, we reported double network (DN) thermoresponsive membranes that incorporated a negatively charged comonomer, 2-acrylamido-2-methylpropane sulfonic acid (AMPS), to improve the mechanical robustness.[46,52] Specifically, these DN hydrogels consist of a tightly cross-linked, negatively charged first network [P(NIPAAm-*co*-AMPS)] containing variable levels of AMPS (NIPAAm:AMPS weight ratio = 100:0 to 25:75) and a loosely cross-linked, interpenetrating second network [PNIPAAm]. In addition, *N*-vinylpyrrolidone (NVP) (∼15 wt % based on NIPAAm weight) was incorporated into the second network to increase the DN VPTT from ∼35 to ∼38 °C. Thus, when implanted into the subcutaneous tissue, this P(NIPAAm-*co*-AMPS)/P(NIPAAm-*co*-NVP) DN membrane would be quite swollen (to maximize glucose diffusion) but cyclical increases/decreases in the temperature of the tissue would cause relative deswelling/reswelling of the membrane to limit cell attachment and to remove adhered cells, as was demonstrated in vitro. Additionally, these membranes demonstrated increased modulus and strength as well as glucose diffusion coefficients (D = 1.8−2.2 × 10^{-6} cm^2/s) in the functional range for dermal and epidermal tissues (D = (2.64 ± 0.42) × 10^{-6} and (0.075 ± 0.05) × 10^{-6} cm^2/s, respectively).[53]

In this work, we sought to house the fluorescent competitive binding assay within the hollow cavity of a cylindrical self-cleaning membrane, toward creating a subcutaneous CGM

DOI: 10.1021/acsabm.8b00267
ACS Appl. Bio Mater. 2018, 1, 1319−1327

with long-term efficacy (Figure 1c). The P(NIPAAm-*co*-AMPS)/P(NIPAAm-*co*-NVP) DN membrane was prepared with a cylindrical geometry (~5 mm × ~2.5 mm, length × diameter), conducive to implantation via simple subcutaneous injection, and with a hollow central cavity (diameter = 600 μm; volume = 1 μL) to house the assay. As shown herein, the mesh size of the membrane exceeded that of the APTS-MT assay component, leading to its rapid leaching from the central cavity. Thus, we evaluated the ability of a layer-by-layer (LbL) coating applied to the surface of the membrane cavity to limit assay diffusion but still permit glucose diffusion. LbL coatings have been explored as semipermeable diffusion barriers on drug-containing microspheres and microcapsules.[54−57] Additionally, LbL coatings have been applied to temporary calcium carbonate microsphere templates containing embedded optical sensing assays for the detection of oxygen, glucose, and urea.[58−61] However, this approach presents challenges in terms of dissolving the template and achieving optimal loading efficiency of the assay. In contrast, the approach reported here, in which the assay is directly housed in a hollow cavity of a membrane rather than loaded onto a template, provides a route for more efficient loading and control of the assay concentration.

Herein we report the use of a LbL coating to inhibit the leaching of a fluorescent competitive binding assay (mPEG-TRITC-ConA/APTS-MT) from the central cavity of a PNIPAAm-based self-cleaning membrane. The negative charge of the P(NIPAAm-*co*-AMPS)/P(NIPAAm-*co*-NVP) DN membrane, stemming from the highly ionized nature of the AMPS comonomer,[62] provided an excellent substrate on which to build a LbL coating. The LbL coating comprised bilayers of positively charged poly(diallyldimethylammonium chloride) ($PDADMAC^+$) and negatively charged poly(sodium 4-styrenesulfonate) (PSS^-). The extent of assay leaching and rate of glucose diffusion as functions of the number of $PDADMAC^+/PSS^-$ bilayers (5, 10, 15, 30, or 40) were investigated. Additionally, biosensors (i.e., assay-loaded membranes) were evaluated for their sensitivity to track glucose levels across a physiological range.

MATERIALS AND METHODS

2.1. Materials. NIPAAm (97%), AMPS (97%), NVP, PEG-DA (~99%; M_n = 575 g/mol), Trizma hydrochloride (Trizma-HCl), manganese(II) chloride ($MnCl_2$), sodium bicarbonate, methyl α-D-mannopyranoside (MaM), $PDADMAC^+$ solution (MW = 100−200 kDa), PSS^- (MW ≈ 70 kDa), and FITC-dextran (MW = 4, 10, 20, or 40 kDa) were obtained from Sigma-Aldrich (St. Louis, MO). Rhodamine B isothiocyanate poly(allylamine hydrochloride) ($RITC\text{-}PAH^+$) was prepared by reacting PAH hydrochloride (MW = 15 kDa) and RITC at a RITC:PAH molar ratio of 20:1 per analogous reports.[63] *N*,*N*′-Methylenebis(acrylamide) (BIS) (99%) was purchased from Acros. 2-Hydroxy-2-methyl-1-phenylpropan-1-one (DAROCUR 1173) was purchased from Ciba Specialty Chemicals (Basel, Switzerland). 1-[4-(2-Hydroxyethoxy)phenyl]-2-hydroxy-2-methylpropan-1-one (Irgacure 2959) was purchased from BASF. Calcium chloride dihydrate ($CaCl_2$) was purchased from J.T. Baker (Center Valley, PA). Sodium chloride (NaCl) was obtained from Mallinckrodt Chemical (St. Louis, MO). Methoxyl-poly-(ethylene glycol)-*N*-hydroxylsuccinimide-succinimidyl carbonate (mPEG-NHS (SC), 5 kDa) was purchased from Nanocs (New York, NY). Anhydrous dextrose (D-glucose) was purchased from Fisher Scientific (Pittsburgh, PA). ConA labeled with tetramethylrhodamine fluorescent dye (TRITC-ConA) and RITC was purchased as a lyophilized powder from Life Technologies (Grand Island, NY). The Tris-buffered saline (TBS) (pH 7.4, 10 mM Trizma-HCl, 0.15 M NaCl, 1 mM $MnCl_2$, and 1 mM $CaCl_2$) and 0.1 M sodium bicarbonate buffer (pH 8.5, 0.15 M NaCl) were prepared with deionized (DI) water (18 MΩ cm). Glass beads (710−850 μm diameter) were purchased from Cospheric LLC (Santa Barbara, CA). The dialysis membrane tubes (20 kDa molecular weight cutoff) were purchased from Spectrum Laboratories (Rancho Dominguez, CA).

2.2. Synthesis of Assay Components. PEGylated-TRITC-ConA and APTS-MT were prepared according to our prior reports.[41,42] In this way, PEGylated-TRITC-ConA was formed with an average of ~5 mPEG chains grafted per ConA monomer.[42]

2.3. Membrane Fabrication. The "first network precursor solution" was formed with NIPAAm and AMPS monomer (NIPAAm:AMPS weight ratio = 75:25, total weight = 1.0 g), BIS cross-linker (0.04 g), Irgacure 2959 photoinitiator (0.08 g), and DI water (7.0 mL). The "second network precursor solution" was formed by combining NIPAAm (6.0 g), NVP (0.96 g), BIS (0.012 g), Irgacure 2959 (0.24 g), and DI water (21.0 mL).

Planar Sheets. Planar sheets (~1.5 mm thickness) were prepared by pipetting the first network precursor solution into a rectangular mold consisting of two glass slides separated by 1 mm thick Teflon spacers. The mold was immersed in an ice−water bath and exposed for 30 min to UV light (UV transilluminator, 6 mW cm^{-2}, 365 nm). The resulting single network (SN) hydrogel was removed from the mold, soaked in DI water for 2 days, and then transferred to the second network precursor to soak for 2 days at 4 °C. The hydrogels were then sandwiched between two glass slides with 1.25 mm thick Teflon spacers enclosing the edges for support. The molds were immersed in an ice−water bath and exposed for 30 min to UV light. The DN hydrogels were removed from the mold and soaked in DI water as before. These specimens were used to measure glucose diffusion.

Hollow Cylindrical Rods. Hollow cylindrical SN rods were prepared by pipetting the first network solution into a cylindrical glass mold (outer diameter = 1 mm, length = 10 mm) fitted with custom Teflon end caps to secure a steel wire (diameter = 300 μm) through the center of the mold and to seal the mold. The mold was immersed in an ice−water bath and exposed for 30 min to UV light as above. To remove the SN hydrogel rods, the Teflon caps were detached, and the molds were heated in an oven (~1 h at 120 °C) to dehydrate and subsequently shrink the rods so that they easily slid out of the mold intact. The SN hydrogels were soaked in DI water for 2 days at room temperature and then transferred into the second network precursor solution for 2 days at 4 °C. Next, a steel wire (~500 μm diameter, representing the new cavity diameter of ~600 μm postswelling) was inserted into the hollow cavity. The construct was wrapped in transparent plastic wrap (Saran), submerged in an ice−water bath, exposed for 10 min to UV light, and finally soaked in DI water as above. The steel wire was removed, and a clean razor blade was used to trim the ends, resulting in hollow rods (5 mm × 2.5 mm × 600 μm, length × outer diameter × inner diameter).

2.4. Membrane Mesh Size. Discs (~13 mm diameter) were harvested from the uncoated hydrogel slabs (~1.5 mm thickness) with a biopsy punch. Each disc was immersed in 0.01 mg/mL FITC-dextran solution for 2 days and then rinsed with DI water, blotted with a Kimwipe, and placed in 1 mL of DI water. The fluorescence intensity of the DI water (due to diffusion of FTIC-dextran from the disc) was monitored at different time points (5 min, 24 h, and 48 h) starting from the time the sample was placed in DI water. The percent intensity ratio (%*I*) was determined by eq 1,

$$\%I = \frac{I_{DI}}{I_{stock}} \times 100\% \quad (1)$$

in which I_{DI} is the intensity of DI water at a given time point and I_{stock} is the intensity of the 0.01 mg/mL stock solution. A %*I* value of <5% indicated that a trace amount of FTIC-dextran could diffuse into the sample, indicating that the particular FTIC-dextran was larger than the hydrogel's mesh size.

2.5. Hydrodynamic Radii of Assay Components. The hydrodynamic radii of PEGylated-TRITC-ConA and APTS-MT

DOI: 10.1021/acsabm.8b00267
ACS Appl. Bio Mater. 2018, 1, 1319−1327

were previously determined to be ~15 and ~1−2 nm, respectively, via dynamic light scattering measurements.[41,42] The hydrodynamic radius of glucose is reported to be ~0.4 nm.[64]

2.6. Deposition of an LbL Coating onto the Inner Cavity Walls of Membrane Rods and onto Planar Slabs. The polyelectrolytes PDADMAC$^+$, PSS$^-$, and RITC-PAH$^+$ were prepared at pH 8 in 5 mM sodium bicarbonate buffer at a concentration of 2 mg/mL. The hollow membrane rod was connected to the inlet and outlet needles (gauge = 30), which were then connected via Teflon tubing (i.d. = $^1/_{32}$″) to a plastic syringe with the designated polyelectrolyte solution or DI water. The syringe was used to dispense 1 mL of solution into the hollow rod cavity, and the solutions were sequentially rinsed through the cavity with short (~1 min) delays between: DI water (5 mL, 3×), positively charged polyelectrolyte (1 mL, 1×), DI water (5 mL, 1×), negatively charged polyelectrolyte (1 mL, 1×) and DI water (5 mL, 1×). After all of the bilayers had been deposited, the cavity was rinsed again with DI water (5 mL, 3×). The portions of the rods that were not coated because the needle was present were cut off, giving a final rod length of 5 mm. Separate rods were deposited with a fluorescently labeled positive layer (RITC-PAH$^+$) instead of PDADMAC$^+$ to image and evaluate the success of the inner wall coating of the polyelectrolytes. For these images, LbL coating (RITC-PAH$^+$/PSS$^-$) of six bilayers was used, and confirmation of the deposition was evaluated with bright-field and fluorescence images (Nikon Eclipse TE2000-U Inverted Microscope, Nikon Instruments, Melville, NY). For all of the other experiments, the LbL coating (PDADMAC$^+$/PSS$^-$) was likewise applied at 5, 15, 30, or 40 bilayers.

LbL-coated planar slabs, designated for glucose diffusion tests, were likewise prepared. Specimens (1 cm × 1 cm) were placed in an open-face filter holder (Pall Co., Port Washington, NY) with one "face" exposed for successive treatment with the designated solutions as described above. The treated specimens were removed and permitted to soak in DI water for 24 h prior to glucose diffusion tests.

2.7. Glucose Diffusion Tests. Planar membrane slabs previously coated LbL with 0, 10, 20, or 30 PDADMAC$^+$/PSS$^-$ bilayers were subjected to glucose diffusion tests performed at 35 °C (i.e., the subcutaneous temperature of the wrist in humans[65]). A specimen (1 cm × 1 cm) was placed in a side-by-side diffusion chamber setup (PermeGear, Bethlehem, PA) with the LbL-coated side facing the receiver chamber containing 3 mL of DI H_2O. The donor chamber contained 3 mL of glucose solution (1000 mg/dL). The chambers were mounted on a stir plate set to 1000 rpm to ensure that the concentrations in both chambers remained uniform. The diffusion chambers were connected to a water bath pump system set to 35 °C. At 20 min intervals for a period of 3 h, 50 μL of solution was extracted from each chamber via a pipet, and the glucose concentration was determined (YSI 2300 Stat Plus biochemistry analyzer, YSI Inc., Yellow Springs, OH).

The diffusion coefficient was calculated using the following derivative form of Fick's second law of diffusion (eq 2):

$$\frac{\partial c}{\partial t} = D\frac{\partial^2 c}{\partial x^2} \tag{2}$$

where c is the concentration within the receiving chamber, t is the time, D is the diffusion coefficient, and x is the diffusion distance.[45,66,67] Under the assumption that each chamber maintained a uniform concentration, eq 2 was simplified to eq 3:[45]

$$Q_t = \frac{ADC_i}{T}\left(t - \frac{T^2}{6D}\right) \tag{3}$$

where Q_t is the amount of glucose transferred through the membrane at a specific time t, A is the area of the hydrogel exposed to either the donor or receiver chamber, C_i is the initial stock glucose concentration within the donor channel at t = 0, and T is the thickness of the hydrogel membrane.

2.8. Assay Leaching from the Assay-Containing Membrane ("Biosensor"). The cavity of a hollow membrane rod (5 mm × 2.5 mm × 600 μm, length × outer diameter × cavity diameter) that had previously been coated with 0, 5, 15, 30, or 40 PDADMAC$^+$/PSS$^-$ bilayers was filled with 1 μL of the glucose sensing assay solution. The assay solution consisted of 10 μM mPEG-TRITC-ConA and 2 μM APTS-MT prepared in TBS. After injection of the assay via the open cavity, each end of the hollow cavity was first capped with a glass bead and then secured by applying ~0.5 μL of a PEG-DA solution (575 g/mol; ~99 wt %) and cured by exposure to UV light (20 s). The sealed rods were thoroughly rinsed with DI water. Each resulting "biosensor" was individually submerged in 150 μL of TBS solution inside a 200 μL PCR centrifuge tube. After 10 min, a small volume of high-concentration glucose solution (glucose dissolved in TBS) was pipetted into the tube to achieve a final glucose concentration of 1000 mg/dL, and the sealed tube (additionally wrapped with Parafilm) was incubated at room temperature. After 24 h, 50 μL of the supernatant surrounding a biosensor was removed and transferred to a microplate reader, and fluorescence measurements were recorded (Tecan microplate reader; excitation wavelength (λ_{ex}) = 450 nm; emission wavelength (λ_{em}) scan range = 480 to 680 nm). The emission peak at ~520 nm was recorded as it pertained to the presence of APTS-MT in the supernatant. Three different biosensors with the designated number of bilayers were used for these measurements.

Next, a more in depth leaching study of both assay components was conducted for biosensors coated LbL with 0 or 30 PDADMAC$^+$/PSS$^-$ bilayers. Biosensors were likewise prepared and individually submerged in 150 μL of glucose solution (1000 mg/dL) inside a 200 μL PCR centrifuge tube. After 1 h, 50 μL of the supernatant surrounding a biosensor was removed and transferred to a microplate reader, and fluorescence measurements were recorded (Tecan microplate reader, λ_{ex} = 450 nm, λ_{em} range = 480 to 680 nm). The peak emissions at ~520 and ~580 nm, indicative of the presence of APTS-MT and PEGylated-TRITC-ConA, respectively, were recorded. The supernatant was then transferred back to the respective PCR tubes. Fluorescence measurements were repeated at times of 2, 3, 4, 5, 8, and 12 h. Three different biosensors with the designated number of bilayers were used for these measurements. To determine the corresponding percent loss of each assay component, 1 μL of the glucose sensing assay solution was pipetted directly into 150 μL of 1000 mg/dL glucose solution in TBS to simulate complete leaching of the assay from the membrane cavity. Then 50 μL of this free assay solution was subjected to fluorescence measurements as above (APTS-MT: λ_{ex} = 450 nm, λ_{em} = 480 to 600 nm, peak $\lambda_{em} \approx$ 520 nm; PEGylated-TRITC-ConA: λ_{ex} = 540 nm, λ_{em} = 560 to 620 nm, peak $\lambda_{em} \approx$ 580 nm). The percent lost was calculated as the ratio of the measured peak emission for each assay component present in the biosensor's supernatant and the initial intensity for each assay component from the above free assay solution measurement.

2.9. Glucose Response of the Assay-Containing Membrane ("Biosensor"). An initial 24 h glucose response study was conducted for biosensors whose hollow cavity was coated LbL with 0, 5, or 30 PDADMAC$^+$/PSS$^-$ bilayers. Each biosensor was individually placed horizontally in a 96-well plate (Greiner Bio-One), and 200 μL of TBS solution was pipetted into each well. After 10 min, fluorescence measurements were recorded (Tecan microplate reader, λ_{ex} = 450 nm, λ_{em} range = 480 to 680 nm), and the FRET ratio (520 nm:600 nm) was recorded as noted above. Next, the biosensor was transferred to a 200 μL PCR centrifuge tube containing 150 μL of high glucose concentration (1000 mg/dL) solution. After 24 h, fluorescence measurements were again taken, and the FRET ratio was likewise recorded. Three different biosensors with the designated number of bilayers were used for these measurements.

Next, a temporal glucose response study was likewise conducted for biosensors whose cavities were coated LbL with 30 PDADMAC$^+$/PSS$^-$ bilayers and exposed to physiologically relevant glucose levels (50−600 mg/dL). A given biosensor was progressively transferred to the well containing a solution of the next highest glucose concentration. After 15 min, the FRET ratio (520 nm:600 nm) was recorded. To determine the percent MARD, the FRET ratio was then plotted as a function of the glucose concentration and fitted to a standard competitive binding curve based on the Boltzmann equation. Three different biosensors were used for these measurements.

DOI: 10.1021/acsabm.8b00267
ACS Appl. Bio Mater. 2018, 1, 1319−1327

2.10. Statistical Analysis. All of the data results are reported as mean ± standard deviation. For each set of data, mean values were compared via GraphPad Prism using analysis of variance (ANOVA) followed by a Tukey post hoc test to determine p values.

RESULTS AND DISCUSSION

Mesh Size of Self-Cleaning DN Membrane. The thermoresponsive, electrostatic P(NIPAAm-*co*-AMPS)/P-(NIPAAm-*co*-NVP) DN membrane was previously shown to exhibit resistance to cell adhesion and accumulation and to display robust mechanical properties.[46,52] The mesh size of the membrane was evaluated herein and determined to be ~6.5 to 10 nm. The hydrodynamic radius of PEGylated-TRITC-ConA (~15 nm)[42] thus exceeds the membrane mesh size, and thus, PEGylated-TRITC-ConA was not anticipated to diffuse from the membrane cavity and through the membrane wall. However, diffusion of APTS-MT would be expected on the basis of its much lower hydrodynamic radius (~1−2 nm).[36] Thus, to prevent leaching of the assay from the hollow cavity of the membrane, we proceeded with application of LbL coatings onto the cavity wall.

Imaging of an LbL Coating Applied to a Membrane Hollow Cavity Wall. To confirm the ability of an LbL coating to line the inner cavity wall of the DN membrane rod, six bilayers of a fluorescently labeled PAH^+ (RITC-PAH^+) and PSS^- were applied. The fluorescence images distinctly confirm the presence of the fluorescent LbL coating (Figure 2). Thus,

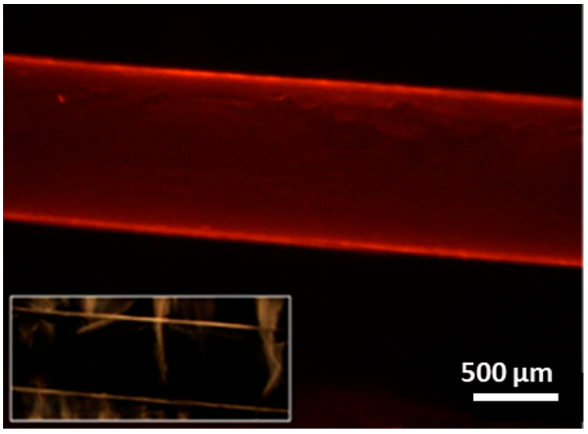

Figure 2. Side-view fluorescent image of a DN membrane cylinder (~600 μm cavity diameter) with a RITC-PAH^+/PSS^- LbL coating applied to the cavity wall (scale bar = 500 μm). The inset is the corresponding bright-field image showing localization of the LbL coating on the cavity wall.

the negative charge stemming from the AMPS comonomer of the DN membrane provided the necessary charged substrate on which the initial, positively charged polyelectrolyte layer (RITC-PAH^+) could be applied, and the LbL coating withstood successive washes with DI water. Moreover, the corresponding bright-field image shows the absence of fluorescence within the middle and outer parts of the walls of the membrane, confirming that the polyelectrolytes did not appreciably diffuse into the membrane walls (Figure 2, inset).

Glucose Diffusion Test. To determine whether the presence of the LbL coatings hindered glucose diffusion, studies were conducted on planar DN membranes coated with 0, 10, 20, or 30 PDADMAC$^+$/PSS^- bilayers. As shown in Figure 3, there were no statistical differences in the measured glucose diffusion coefficients. This is attributed to the small hydrodynamic radius of glucose (~0.4 nm).[64]

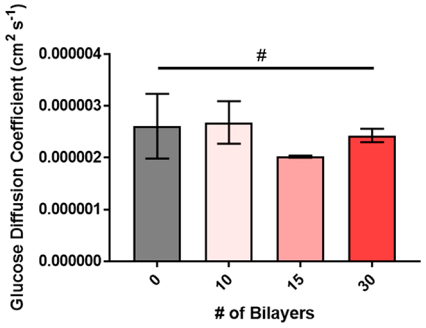

Figure 3. Glucose diffusion coefficients of DN membranes coated with varying numbers of PDADMAC$^+$/PSS^- bilayers. #, $p > 0.05$.

Leaching of APTS-MT versus Number of Bilayers. Biosensors were created by coating the hollow cavities of DN membrane rods with 0, 5, 15, 30, or 40 PDADMAC$^+$/PSS^- bilayers and subsequently filling the cavities with 1 μL of the glucose sensing assay solution. Each biosensor was submerged in a solution with a high glucose concentration (1000 mg/dL). This high concentration of glucose leads to the unbound states of PEGylated-TRITC-ConA and APTS-MT (Figure 1a) and thus maximizes the potential of assay components to diffuse through the membrane. As noted above, in the unbound state only APTS-MT was expected to be able to diffuse through the membrane. Thus, for initial fluorescence measurements of the liquid surrounding each biosensor, the emission peak at ~520 nm was recorded at 24 h to detect APTS-MT that had leached from the cavity (Figure 4). The fluorescence intensity of APTS

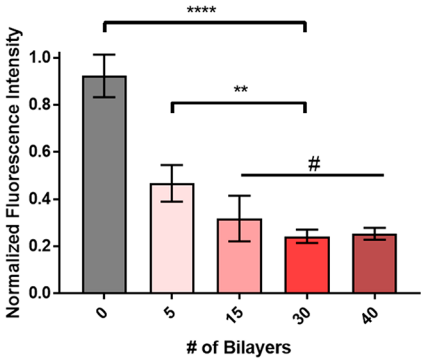

Figure 4. Normalized fluorescence (λ_{em} ≈ 520 nm) due to APTS of APTS-MT in the supernatant surrounding assay-filled biosensors following 24 h exposure to a solution with a high glucose concentration (1000 mg/dL). ****, $p < 0.0001$; **, p = 0.001−0.01; #, $p > 0.05$.

in the supernatant surrounding the biosensor progressively decreased as the number of PDADMAC$^+$/PSS^- bilayers increased from 5 to 15 and 30 but did not decrease significantly further with 40 bilayers.

On the basis of their superior retention of the APTS-MT assay component, biosensors with 30 bilayers were evaluated intermittently over a period of 12 h when exposed to 1000 mg/dL glucose solution. The fluorescence at both λ_{em} ≈ 520 nm and λ_{em} ≈ 580 nm from the supernatant surrounding a biosensor were recorded to detect the presence of APTS-MT

DOI: 10.1021/acsabm.8b00267
ACS Appl. Bio Mater. 2018, 1, 1319−1327

and PEGylated-TRITC-ConA, respectively. On the basis of a hydrodynamic radius (~15 nm) that exceeds the membrane's mesh size (~6.5 to 10 nm), mPEG-TRITC-ConA was retained even in the absence of the LbL coating (Figure 5a).

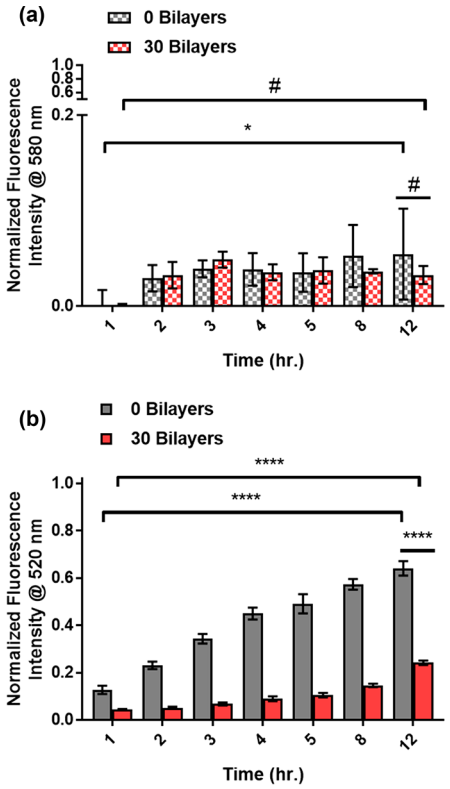

Figure 5. Cumulative fluorescence of the supernatant surrounding assay-filled biosensors (whose cavities were coated with 0 or 30 bilayers) during 12 h exposure to a solution of high glucose concentration (1000 mg/dL): (a) normalized fluorescence ($\lambda_{em} \approx$ 580 nm) due to TRITC of PEGylated-TRITC-ConA and (b) normalized fluorescence ($\lambda_{em} \approx$ 520) due to APTS of APTS-MT. ****, $p < 0.0001$; *, $p = 0.01-0.05$; #, $p > 0.05$.

Over all of the time points, it was calculated that less than 6% of the PEGylated-TRITC-ConA housed in the biosensor cavity had leached through the membrane wall and into the surrounding supernatant. In contrast, because of its very low hydrodynamic radius (~1−2 nm), APTS-MT readily diffused from the uncoated biosensor cavity, with the level increasing progressively over 12 h (Figure 5b). This diffusion resulted in losses of 13% and 64% of APTS-MT at 1 and 12 h, respectively. However, for a biosensor whose cavity was coated with 30 bilayers, diffusion of APTS-MT was substantially diminished, leading to losses of 4% and 24% after 1 and 12 h.

Glucose Response of Biosensors. The potential impact of the LbL coating on the glucose responsivity of the biosensor was initially evaluated by comparing the FRET ratios of biosensors with no bilayers ("0 bilayers") and low ("5 bilayers") and high ("30 bilayers") numbers of bilayers applied to the cavity wall before and after 24 h exposure to a solution with a high glucose concentration (Figure 6). Upon exposure to a high glucose level, the FRET response of the assay system should increase (Figure 1a). However, for biosensors with 0 or 5 bilayers, this was not observed. On the basis of the glucose diffusion studies, an LbL coating (even at 30 bilayers) does not inhibit glucose diffusion through the membrane (Figure 3).

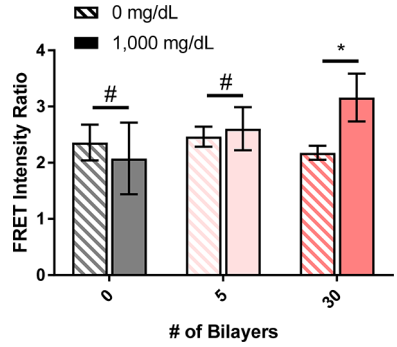

Figure 6. FRET intensity ratios of assay-filled biosensors whose cavities were coated with 0, 5, or 30 bilayers upon exposure to 0 or 1000 mg/dL glucose solutions for 24 h. *, $p = 0.01-0.05$; #, $p > 0.05$.

Thus, this compromised FRET response can be attributed to the loss of APTS-MT from the biosensors whose cavities were coated with 0 or 5 bilayers (Figures 4 and 5b). In contrast, because of its retention of APTS-MT, a biosensor whose cavity was coated with 30 bilayers exhibited the expected increase in FRET response.

Because of its retention of APTS-MT and subsequent increased FRET response to high glucose levels, biosensors with 30 bilayers were sequentially exposed to increasing physiologically relevant glucose concentrations (50 to 600 mg/dL) for 15 min intervals (Figure 7). Across this range, the

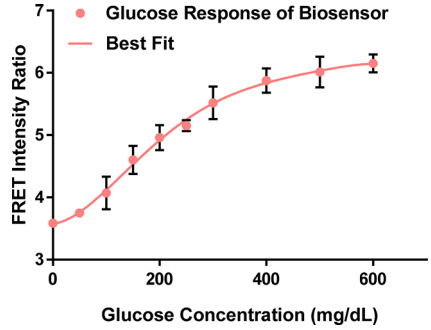

Figure 7. FRET intensity ratio of assay-filled biosensors whose cavities were coated with 30 bilayers upon exposure to increasing physiologically relevant glucose concentrations (0 to 600 mg/dL) for 15 min intervals.

biosensors exhibited the expected progressive increase in FRET response, indicating their responsivity to different glucose levels after only short time intervals.

For these biosensors with 30 bilayers, the % MARD was determined by plotting the FRET ratio as a function of the glucose concentration and fitting to a standard competitive binding curve (Figure 8). The results indicated that these biosensors are able to track changes in glucose concentration across the physiologic range with a MARD of 11 ± 0.9%. Our group has previously reported that the glucose response of this assay in free solution resulted in a MARD of ~5% across a physiological relevant glucose range.[43] While the % MARD increased upon housing of the assay in the biosensor cavity, this is expected because glucose must now diffuse across the membrane wall to reach the assay.

DOI: 10.1021/acsabm.8b00267
ACS Appl. Bio Mater. 2018, 1, 1319−1327

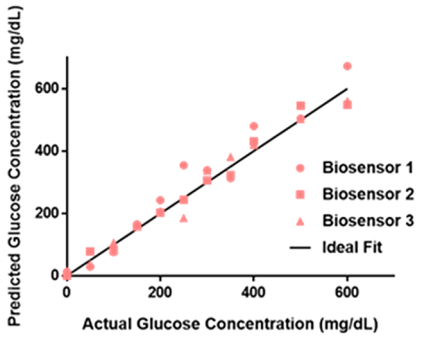

Figure 8. Predicted versus actual glucose response of three assay-filled biosensors whose cavities were coated with 30 bilayers, corresponding to a calculated MARD of ∼11%.

CONCLUSIONS

Toward the development of a CGM with an extended lifetime and the ability to be implanted fully subcutaneously, we have reported the incorporation of a fluorescent competitive binding glucose sensing assay within the central cavity of a cylindrical "self-cleaning" membrane. The assay comprised PEGylated-TRITC-ConA and APTS-MT, and the membrane was a thermoresponsive, electrostatic P(NIPAAm-*co*-AMPS)/P-(NIPAAm-*co*-NVP) DN hydrogel. Of central importance was reducing the leaching of the assay from the membrane cavity. Therefore, an LbL coating comprising $PDADMAC^{+}/PSS^{-}$ bilayers was applied to the biosensor cavity walls. The negatively charged nature of the membrane imparted by the AMPS comonomer provided a suitable substrate for the LbL coating. The membrane's determined mesh size (∼6.5 to 10 nm) indicated that the necessary diffusion of glucose (∼0.4 nm) would not be inhibited and that undesired assay component leaching would not be expected for PEGylated-TRITC-ConA (∼15 nm) but would be for APTS-MT (∼1−2 nm). Indeed, even a 30 bilayer LbL coating was shown not to diminish glucose diffusion, and PEGylated-TRITC-ConA leaching was limited (<6%) for even uncoated membranes. However, uncoated membrane cavities permitted the loss of 64% of APTS-MT (under high glucose concentration conditions) in just 12 h. When the cavity was coated with 30 bilayers, loss of APTS-MT from the cavity was reduced to 24%. Such biosensors also exhibited the expected increase in FRET response upon successive exposure to increasing concentrations of glucose (50 to 600 mg/dL) over brief time intervals (15 min). Moreover, these biosensors were able to track changes in physiological glucose concentrations with a MARD of 11 ± 0.9%. Thus, an LbL coating shows potential to realize the effective housing of this optical glucose sensing assay in a self-cleaning membrane. Further refinement of the LbL coating or the membrane mesh size (e.g., through cross-linking density) may afford further diminished assay diffusion.

AUTHOR INFORMATION

Corresponding Author

*E-mail: mgrunlan@tamu.edu.

ORCID

Melissa A. Grunlan: 0000-0002-5428-0461

Notes

The authors declare no competing financial interest.

ACKNOWLEDGMENTS

The authors thank Dr. Ashvin Nagaraja (Texas A&M University) and Prof. Gyula Vigh (Texas A&M University) for assisting with the preparation of RITC-PAH and APTS-MT, respectively. Funding from the NIH/NIDDK (1R01DK095101-01A1) is gratefully acknowledged. This work was supported in part by funding from the National Science Foundation Engineering Research Center for Precise Advanced Technologies and Health Systems for Underserved Populations (PATHS-UP) (Award 1648451).

REFERENCES

(1) American Diabetes Association. Diabetes Basics. http://www.diabetes.org/diabetes-basics/ (accessed June 25, 2018).
(2) American Diabetes Association. Economic Costs of Diabetes in the U.S. in 2012. *Diabetes Care* **2013**, *36*, 1033−1046.
(3) Bode, B.; Battelino, T. Continuous Glucose Monitoring. *Int. J. Clin. Pract.* **2010**, *64*, 11−15.
(4) Beck, R. W.; et al. The Effect of Continuous Glucose Monitoring in Well-controlled Type 1 Diabetes. *Diabetes Care* **2009**, *32*, 1378−1383.
(5) Klonoff, D. C. Continuous Glucose Monitoring Roadmap for 21st Century Diabetes Therapy. *Diabetes Care* **2005**, *28*, 1231−1239.
(6) Damiano, E. R.; El-Khatib, F. H.; Zheng, H.; Nathan, D. M.; Russell, S. J. A Comparative Effectiveness Analysis of Three Continuous Glucose Monitors. *Diabetes Care* **2013**, *36*, 251−259.
(7) McNichols, R. J.; Coté, G. L. Optical Glucose Sensing in Biological Fluids: An Overview. *J. Biomed. Opt.* **2000**, *5*, 5−16.
(8) Oliver, N. S.; Toumazou, C.; Cass, A. E. G.; Johnston, D. G. Glucose Sensors: A Review of Current and Emerging Technology. *Diabetic Med.* **2009**, *26*, 197−210.
(9) Wang, J. Glucose Biosensors: 40 Years of Advances and Challenges. *Electroanalysis* **2001**, *13*, 983−988.
(10) Shafer-Peltier, K. E.; Haynes, C. L.; Glucksberg, M. R.; Van Duyne, R. P. Toward a Glucose Biosensor based on Surface-enhanced Raman Scattering. *J. Am. Chem. Soc.* **2003**, *125*, 588−593.
(11) Barman, I.; Kong, C. R.; Dingari, N. C.; Dasari, R. R.; Feld, M. S. Development of Robust Calibration Models Using Support Vector Machines for Spectroscopic Monitoring of Blood Glucose. *Anal. Chem.* **2010**, *82*, 9719−9726.
(12) Enejder, A. M.; Scecina, T. G.; Oh, J.; Hunter, M.; Shih, W. C.; Sasic, S.; Horowitz, G. L.; Feld, M. S. Raman Spectroscopy for Noninvasive Glucose Measurements. *J. Biomed. Opt.* **2005**, *10*, 031114.
(13) Lambert, J. L.; Morookian, J. M.; Sirk, S. J.; Borchert, M. S. Measurement of Aqueous Glucose in a Model Anterior Chamber Using Raman Spectroscopy. *J. Raman Spectrosc.* **2002**, *33*, 524−529.
(14) Qi, D.; Berger, A. J. Chemical Concentration Measurement in Blood Serum and Urine Samples Using Liquid-core Optical Fiber Raman Spectroscopy. *Appl. Opt.* **2007**, *46*, 1726−1734.
(15) Esenaliev, R. O.; Larin, K. V.; Larina, I. V.; Motamedi, M. Noninvasive Monitoring of Glucose Concentration with Optical Coherence Tomography. *Opt. Lett.* **2001**, *26*, 992−994.
(16) Sapozhnikova, V. V.; Prough, D.; Kuranov, R. V.; Cicenaite, I.; Esenaliev, R. O. Influence of Osmolytes on *in vivo* Glucose Monitoring Using Optical Coherence Tomography. *Exp. Biol. Med.* **2006**, *231*, 1323−1332.
(17) MacKenzie, H. A.; Ashton, H. S.; Shen, Y. C.; Lindberg, J.; Rae, P.; Quan, K. M.; Spiers, S. Blood Glucose Measurements by Photoacoustics. *OSA Trends Opt. Photonics* **1998**, *22*, BTuC1.
(18) Weiss, R.; Yegorchikov, Y.; Shusterman, A.; Raz, I. Noninvasive Continuous Glucose Monitoring Using Photoacoustic Technology - Results from the First 62 Subjects. *Diabetes Technol. Ther.* **2007**, *9*, 68−74.
(19) Zeng, L.; Liu, G.; Yang, D.; Ren, Z.; Huang, Z. Design of a Portable Noninvasive Photoacoustic Glucose Monitoring System

DOI: 10.1021/acsabm.8b00267
ACS Appl. Bio Mater. 2018, 1, 1319−1327

Integrated Laser Diode Excitation with Annular Array Detection. *Proc. SPIE* **2009**, *7280*, 72802F.
(20) Ansari, R. R.; Böckle, S.; Rovati, L. New Optical Scheme for a Polarimetric-based Glucose Sensor. *J. Biomed. Opt.* **2004**, *9*, 103−115.
(21) Cameron, B. D.; Anumula, H. Development of a Real-time Corneal Birefringence Compensated Glucose Sensing Polarimeter. *Diabetes Technol. Ther.* **2006**, *8*, 156−164.
(22) Cameron, B. D.; Baba, J. S.; Coté, G. L. Measurement of the Glucose Transport Time Delay Between the Blood and Aqueous Humor of the Eye for the Eventual Development of a Noninvasive Glucose Sensor. *Diabetes Technol. Ther.* **2001**, *3*, 201−207.
(23) Malik, B. H.; Coté, G. L. Real-Time Dual Wavelength Polarimetry for Glucose Sensing. *Proc. SPIE* **2009**, *7186*, 718604.
(24) Wan, Q.; Coté, G. L.; Dixon, J. B. Dual-Wavelength Polarimetry for Monitoring Glucose in the Presence of Varying Birefringence. *J. Biomed. Opt.* **2005**, *10*, 024029.
(25) Burmeister, J. J.; Arnold, M. A.; Small, G. W. Noninvasive Blood Glucose Measurements by Near-infrared Transmission Spectroscopy Across Human Tongues. *Diabetes Technol. Ther.* **2000**, *2*, 5−16.
(26) Vrancic, C.; Fomichova, A.; Gretz, N.; Herrmann, C.; Neudecker, S.; Pucci, A.; Petrich, W. Continuous Glucose Monitoring by means of Mid-infrared Transmission Laser Spectroscopy *in vitro*. *Analyst* **2011**, *136*, 1192−1198.
(27) McShane, M. J. Potential for Glucose Monitoring with Nanoengineered Fluorescent Biosensors. *Diabetes Technol. Ther.* **2002**, *4*, 533−538.
(28) Ballerstadt, R.; Polak, A.; Beuhler, A.; Frye, J. *In vitro* Long-term Performance Study of a Near-infrared Fluorescence Affinity Sensor for Glucose Monitoring. *Biosens. Bioelectron.* **2004**, *19*, 905−914.
(29) D'Auria, S.; Di Cesare, N.; Gryczynski, Z.; Gryczynski, I.; Rossi, M.; Lakowicz, J. R. A thermophilic Apoglucose Dehydrogenase as Nonconsuming Glucose Sensor. *Biochem. Biophys. Res. Commun.* **2000**, *274*, 727−731.
(30) Siegrist, J.; Kazarian, T.; Ensor, C.; Joel, S.; Madou, M.; Wang, P.; Daunert, S. Continuous Glucose Sensor Using Novel Genetically Engineered Binding Polypeptides Towards *in vivo* Applications. *Sens. Actuators, B* **2010**, *149*, 51−58.
(31) Tolosa, L.; Malak, H.; Raob, G.; Lakowicz, J. R. Optical Assay for Glucose Based on the Luminescnence Decay Time of the Long Wavelength. *Sens. Actuators, B* **1997**, *45*, 93−99.
(32) Schultz, J. S.; Mansouri, S.; Goldstein, I. J. Affinity sensor: A New Technique for Developing Implantable Sensors for Glucose and Other Metabolites. *Diabetes Care* **1982**, *5*, 245−253.
(33) Ballerstadt, R.; Schultz, J. S. A Fluorescence Affinity Hollow Fiber Sensor for Continuous Transdermal Glucose Monitoring. *Anal. Chem.* **2000**, *72*, 4185−4192.
(34) Ibey, B. L.; Beier, H. T.; Yadavalli, V. K.; Rounds, R. M.; Pishko, M. V.; Coté, G. L. Competitive Binding Assay For Glucose Based on Glycodendrimer-fluorophore Conjugates. *Anal. Chem.* **2005**, *77*, 7039−7046.
(35) Liao, K.-C.; Hogen-Esch, T.; Richmond, F. J.; Marcu, L.; Clifton, W.; Loeb, G. E. Percutaneous Fiber-optic Sensor for Chronic Glucose Monitoring in vivo. *Biosens. Bioelectron.* **2008**, *23*, 1458−1465.
(36) Cummins, B. M.; Lim, J.; Simanek, E. E.; Pishko, M. V.; Coté, G. L. Encapsulation of a Concanavalin A/dendrimer Glucose Sensing Assay within Microporated Poly(ethylene glycol) Microspheres *BIomed. Biomed. Opt. Express* **2011**, *2*, 1243−1257.
(37) Russell, R. J.; Pishko, M. V.; Gefrides, C. C.; McShane, M. J.; Coté, G. L. A Fluorescence-based Glucose Biosensor Using Concanavalin A and Dextran Encapsulated in a Poly(ethylene glycol) Hydrogel. *Anal. Chem.* **1999**, *71*, 3126−3132.
(38) *Concanavalin A as a Tool*; Bittiger, H., Schnebli, H. P., Eds.; John Wiley & Sons: London, 1976.
(39) Ehwald, R.; Ballerstädt, R.; Dautzenberg, H. Viscosimetric Affinity Assay. *Anal. Biochem.* **1996**, *234*, 1−8.
(40) McCartney, L. J.; Pickup, J. C.; Rolinski, O. J.; Birch, D. J. S. Near-Infrared Fluorescence Lifetime Assay for Serum Glucose Based on Allophycocyanin-Labeled Concanavalin A. *Anal. Biochem.* **2001**, *292*, 216−221.
(41) Cummins, B. M.; Li, M.; Locke, A. K.; Birch, D. J. S.; Vigh, G.; Coté, G. L. Overcoming the Aggregation Problem: A New Type of Fluorescent Ligand for ConA-based Glucose Sensing. *Biosens. Bioelectron.* **2015**, *63*, 53−60.
(42) Locke, A. K.; Cummins, B. M.; Abraham, A. A.; Coté, G. L. PEGylation of Concanavalin A to Improve Its Stability for An *in vivo* Glucose Sensing Assay. *Anal. Chem.* **2014**, *86*, 9091−9097.
(43) Locke, A. K.; Cummins, B. M.; Coté, G. L. High Affinity Mannotetraose as an Alternative to Dextran in ConA Based Fluorescent Affinity Glucose Assay Due to Improved FRET Efficiency. *ACS Sensors* **2016**, *1*, 584−590.
(44) Gant, R.; Hou, Y.; Grunlan, M. A.; Coté, G. L. Development of a Self-Cleaning Sensor Membrane for Implantable Biosensors. *J. Biomed. Mater. Res., Part A* **2009**, *90A*, 695−701.
(45) Abraham, A. A.; Fei, R.; Coté, G. L.; Grunlan, M. A. Self-cleaning Membrane to Extend the Lifetime of An Implanted Glucose Biosensor. *ACS Appl. Mater. Interfaces* **2013**, *5*, 12832−12838.
(46) Fei, R.; Means, A. K.; Abraham, A. A.; Locke, A. K.; Coté, G. L.; Grunlan, M. A. Self-cleaning, Thermoresponsive P(NIPAAm-*co*-AMPS) Double Network Membranes for Implanted Glucose Biosensors. *Macromol. Mater. Eng.* **2016**, *301*, 935−943.
(47) Huffman, A. S.; Afrassiabi, A.; Dong, L. C. Thermally Reversible Hydrogels: II. Delivery and Selective Removal of Substances from Aqueous Solution. *J. Controlled Release* **1986**, *4*, 213−222.
(48) Zhang, J.; Pelton, R.; Deng, Y. Temperature-dependent Contact Angles of Water on Poly(*N*-isopropylacrylamide) Gels. *Langmuir* **1995**, *11*, 2301−2302.
(49) Okano, T.; Yamada, N.; Okuhara, M.; Sakai, H.; Sakurai, Y. Mechanism of Cell Detachment from Temperature-modulated, Hydrophilic-hydrophobic Polymer Surfaces. *Biomaterials* **1995**, *16*, 297−303.
(50) Yamato, M.; Akiyama, Y.; Kobayashi, J.; Yang, J.; Kikuchi, A.; Okano, T. Temperature-responsive Cell Culture Surfaces for Regenerative Medicine with Cell Sheet Engineering. *Prog. Polym. Sci.* **2007**, *32*, 1123−1133.
(51) Kobayashi, J.; Okano, T. Fabrication of a Thermoresponsive Cell Culture Dish: A Key Technology for Cell Sheet Tissue Engineering. *Sci. Technol. Adv. Mater.* **2010**, *11*, 014111.
(52) Fei, R.; George, J. T.; Park, J.; Means, A. K.; Grunlan, M. A. Ultra-strongThermoresponsive Double Network Hydrogels. *Soft Matter* **2013**, *9*, 2912−2919.
(53) Khalil, E.; Kretsos, K.; Kasting, G. B. Glucose Partition Coefficient and Diffusivity in the Lower Skin Layers. *Pharm. Res.* **2006**, *23*, 1227−1234.
(54) Decher, G.; Hong, J. D.; Schmitt, J. Buildup of Ultrathin Multilayer Films by a Self-Assembly Process: III. Consecutively Alternating Adsorption of Anionic and Cationic Polyelectrolytes on Charged Surfaces. *Thin Solid Films* **1992**, *210-211*, 831−835.
(55) Iost, R. M.; Crespilho, F. N. Layer-by-layer Self-assembly and Electrochemistry: Applications in Biosensing and Bioelectronics. *Biosens. Bioelectron.* **2012**, *31*, 1−10.
(56) Tong, W.; Song, X.; Gao, C. Layer-by-layer Assembly of Microcapsules and Their Biomedical Applications. *Chem. Soc. Rev.* **2012**, *41*, 6103−6124.
(57) Swati, M.; Srivastava, R. Polyelectrolyte-Coated Alginate Microspheres for Optical Urea Sensing. In *Proceedings of the 2009 9th IEEE Conference on Nanotechnology (IEEE NANO)*; IEEE: New York, 2010; pp 846−849.
(58) Stein, E. W.; Volodkin, D. V.; McShane, M. J.; Sukhorukov, G. B. Real-time Assessment of Spatial and Temporal Coupled Catalysis within Polyelectrolyte Microcapsules Containing Coimmobilized Glucose Oxidase and Peroxidase. *Biomacromolecules* **2006**, *7*, 710−719.

DOI: 10.1021/acsabm.8b00267
ACS Appl. Bio Mater. 2018, 1, 1319−1327

(59) Sato, K.; Takahashi, S.; Anzai, J. Layer-by-layer Thin Films and Microcapsules for Biosensors and Controlled Release. *Anal. Sci.* **2012**, *28*, 929−938.
(60) Chinnayelka, S.; McShane, M. J. Glucose Sensors Based on Microcapsules Containing an Orange/red Competitive Binding Resonance Energy Transfer Assay. *Diabetes Technol. Ther.* **2006**, *8*, 269−278.
(61) Chinnayelka, S.; Zhu, H.; McShane, M. Near-Infrared Resonance Energy Transfer Glucose Biosensors in Hybrid Microcapsule Carriers. *J. Sens.* **2008**, *2008*, 346016.
(62) Travas-Sejdic, J.; Easteal, A. Swelling Equilibria and Volume Phase Transition of Polyelectrolyte Gel with Strongly Dissociated Groups. *Polym. Gels Networks* **1998**, *5*, 481−502.
(63) Reibetanz, U.; Lessig, J.; Hoyer, J.; Neundorf, I. Surface Functionalized Colloidal Microparticles for Fast Endocytotic Cell Uptake. *Adv. Eng. Mater.* **2010**, *12*, B488−B495.
(64) Schultz, S. G.; Solomon, A. K. Determination of the Effective Hydrodynamic Radii of Small Molecules by Viscometry. *J. Gen. Physiol.* **1961**, *44*, 1189−1199.
(65) Werner, J.; Buse, M. Temperature Profiles with Respect to Inhomogeneity and Geometry of the Human Body. *J. Appl. Physiol.* **1988**, *65*, 1110−1118.
(66) Zhang, W.; Furusaki, S. On the Evaluation of Diffusivities in Gels Using the Diffusion Cell Technique. *Biochem. Eng. J.* **2001**, *9*, 73−82.
(67) Teixeira, J.; Mota, M.; Venâncio, A. Model Identification and Diffusion Coefficients Determination of Glucose and Malic Acid in Calcium Alginate Membranes. *Chem. Eng. J. and Biochem. Eng. J.* **1994**, *56*, B9−B14.

DOI: 10.1021/acsabm.8b00267
ACS Appl. Bio Mater. 2018, 1, 1319−1327